Proton Spectra from the $p+D$ Reaction for 5–10 MeV Incident Protons*†

JOSEPH L. FRIEDES‡ AND MORTON K. BRUSSEL
University of Illinois, Urbana, Illinois
(Received 19 March 1963)

The proton spectra from the $p+D \rightarrow 2p+n$ reaction have been measured at the four laboratory energies, 10.62, 9.19, 6.97, and 5.53 MeV, and at the two laboratory angles, 14° and 34°. The proton beam from the University of Illinois cyclotron was used to bombard a deuterated polyethylene target. The breakup protons were recorded by a thin CsI scintillation counter used in conjunction with a magnetic spectrometer. The energy resolution of the system was approximately one percent and the minimum energy for which reliable data could be obtained was 1 MeV. All of the spectra have fewer low-energy protons than would be predicted by phase-space arguments alone. They all exhibit rather steep slopes near the maximum breakup energy, reaching one-third to one-half maximum height in less than $\frac{1}{4}$ MeV. The slope then decreases, the cross section rising to a maximum near $E/E_{\max}=\frac{1}{2}$. Structure, in the form of a "knee" in the spectrum, has been observed near the maximum breakup energy for all the spectra with incident proton energies greater than 7 MeV. This structure becomes more pronounced as the scattering angle increases and less pronounced as the incident energy decreases. Similar structure has also been observed near the low-energy end of the spectrum for the 10.6-MeV incident proton energy. The present observations have been compared with the less complete work of other investigators, and the agreement was found to be excellent. A qualitative understanding of the observed structure is provided by the final-state interaction formalism of Watson. A comparison with the impulse approximation theory of Frank and Gammel has also been made and the agreement is rather poor.

I. INTRODUCTION

THE breakup reactions $p+D \rightarrow 2p+n$ and $n+D \rightarrow 2n+p$ are among the simplest inelastic nuclear reactions and as such are worthy of intensive experimental and theoretical study. At present, their primary theoretical importance probably arises more as a test of the validity of the approximations used in the calculation of the cross section than as a means of probing the detailed nature of the forces involved in the interaction.

The neutron spectra[1] from the $p+D \rightarrow 2p+n$ reaction have been studied extensively by Ferguson and Morrison,[2] Cranberg and Smith[3] and Wong *et al.*[4] The neutrons from this reaction can be roughly classified into a fast and a slow group. The slow group is a result of the direct scattering of the incident proton by one of the nucleons in the deuteron, just enough energy being transferred to the deuteron to disassociate it. The resulting neutron emission is approximately isotropic. The high-energy neutron group arises either from a direct knockout process or from a charge-exchange interaction between the incident proton and the neutron in the deuteron. The energy spectrum might, therefore, be expected to have two peaks, the high-energy peak disappearing as the scattering angle is increased. The experimental results have these general characteristics. Recently, Ilakovac *et al.*[5] observed a similar spectrum for the protons from the $n+D$ reaction.

Bransden and Burhop[6] have made the most extensive calculations of the breakup spectrum. They used the distorted-wave approximation which, in its most general form, involves the calculation of matrix elements using wave functions which represent the motion of the nucleon in the mean field of the deuteron in the initial state and in the mean field of the excited or "virtual deuteron" in the final state. Bransden and Burhop neglect the distortion of the outgoing wave in the final state, and use a plane wave to describe the relative motion of the outgoing nucleon with respect to the other two. Therefore, it is not surprising to find that their results disagree with the experiments, and even predict, for 10-MeV incident protons, a total cross section for breakup eight times larger than the theoretical maximum for S-wave interactions.

Frank and Gammel[7] have developed a theory using the impulse approximation, in which it is possible to express the inelastic cross section in terms of the known elastic cross sections of the nucleon-nucleon interaction. In order to obtain the results in a closed form, they used zero-range potentials, and the reasonable agreement of their calculations with the total cross-section data of Allred *et al.*[8] and the 4-MeV spectra of Ferguson and Morrison[2] is probably fortuitous. Frank and Gammel only considered the contribution from the n-p final states, and therefore it is not surprising to find that the

* Supported in part by the U. S. Office of Naval Research.
† This work is described in greater detail in a thesis submitted to the University of Illinois by J. L. Friedes in partial fulfillment of the requirements for the Ph.D. degree.
‡ Present address: Department of Physics, Brookhaven National Laboratory, Upton, New York.
[1] The following terminology will be used. Let θ be the angle of observation, and E the energy of the observed nucleon. Then $d^2\sigma(\theta,E)/d\Omega dE$ is the "differential cross section," $d\sigma(\theta)/d\Omega = \int (d^2\sigma/d\Omega dE)\, dE$ is the "cross section," and $\sigma = \int [d\sigma(\theta)/d\Omega]\, d\Omega$ is the "total cross section." The breakup "spectrum" is a measurement of $d^2\sigma(\theta,E)/d\Omega dE$ versus E.
[2] A. Ferguson and G. Morrison, Nucl. Phys. **5**, 41 (1958).
[3] L. Cranberg and R. Smith, Phys. Rev. **113**, 587 (1959).
[4] C. Wong, J. Anderson, C. Gardner, J. McClure, and M. Nakada, Phys. Rev. **116**, 164 (1959).
[5] K. Ilakovac, L. Kuo, M. Petravic, I. Slaus, and P. Thomas, Phys. Rev. Letters **6**, 356 (1961).
[6] B. Bransden and E. Burhop, Proc. Phys. Soc. (London) **A63**, 1937 (1950).
[7] R. Frank and J. Gammel, Phys. Rev. **93**, 463 (1954).
[8] J. Allred, A. Armstrong, and L. Rosen, Phys. Rev. **91**, 90 (1953).

high-energy neutron peak observed by Cranberg and Smith and Wong *et al.* is not reproduced by their theory.

Heckrotte and MacGregor[9] have extended the theory of Frank and Gammel and have shown that the high-energy peak may be explained by the interaction of the two identical nucleons in the final state. Since they, too, use the Born approximation, their results are only qualitatively correct, the value of the cross section being in error by an order of magnitude. Komarov and Popova[10] have carried out similar calculations in which they considered the three final-state interaction regions (p-p; no dominant final state; n-p) separately. The agreement that they obtained with the experimental data is excellent, but somewhat arbitrary because of their normalization procedures.

The effect of these final-state interactions on the shape of the energy spectrum of the emitted particles was first considered by Migdal[11] and subsequently by Watson.[12] Peaks ascribed to final-state interactions have been observed by Rybakov *et al.*[13] in the d-D, d-He^3, and d-He^4 breakup reactions. Qualitative fits to the data were obtained using the simple theory of Migdal.

Although all of the calculations mentioned above indicate that the general structure of the breakup spectrum can be explained on the basis of final-state interactions, a completely satisfactory theory which gives the correct magnitude and shape does not exist at the present time.

The Present Experiment

Prior to 1960, only the neutron (proton) spectrum from the $p+D$ ($n+D$) reaction had been measured. The proton spectrum from the $p+D$ reaction has since been observed by Kikuchi *et al.*[14] and by Nisimura.[15] Their experimental arrangement limited their energy resolution to approximately 10% and the minimum detectable proton energy to 3 MeV. A factor of 10 improvement in the energy resolution and a minimum detectable proton energy of less than 1 MeV has been achieved in the present experiment by using a magnetic spectrometer to observe the breakup protons. The proton spectrum has been measured at two laboratory angles, 14° and 34°, and four energies, 5.53, 6.97, 9.19, and 10.62 MeV.

II. EXPERIMENTAL EQUIPMENT

The main experimental difficulties associated with measuring the breakup spectrum are due to: (1) a general background from neutrons and gamma rays, and from protons which are degraded in energy by slit scattering, and (2) elastically scattered deuterons which have the same energy as the protons from the deuteron breakup. The neutron-gamma-ray background was reduced by use of a magnetic spectrometer with a thin (0.005-in.) CsI scintillation counter to detect the desired protons. This apparatus removes the detector from near the target and also allows deuterons to be distinguished from protons.

Figure 1 is a schematic drawing of the essential equipment. The proton beam from the University of Illinois spiral ridge cyclotron, collimated by slits S_3, S_4, and S_5 to a 0.125-in.×0.125-in. square cross section, passes through the target and is collected by a conventional type Faraday cup. The antiscattering shield prevents particles scattered by S_3 from directly reaching the counters. The monitor counter is used to detect the elastically scattered protons. Slits S_1 and S_2 determine the magnet counter solid angle, and slit S_6 determines the monitor counter solid angle.

The spectrometer is of the Browne-Buechner type[16] and possesses an energy resolution capability of better than 0.1%. The momentum calibration, dispersion, and magnification of the spectrometer were measured using the alpha-particle sources Po^{210}(5.302-MeV alpha particles) and Bi^{212}(6.047-, 6.086-, and 8.780-MeV alpha particles). All of the measurements were consistent with the geometrical calculations. The magnetic field was determined by a proton resonance (NMR) device.

The $(CD_2)_n$ target used in this experiment was prepared from crystalline $(CD_2)_n$ in a manner similar to that described by Reid.[17] The yield of protons elastically scattered from the deuterium was measured and compared with the results of Allred *et al.*[18] who employed a gas target. In this way, the thickness was determined to be 1.31 ± 0.08 mg/cm². This target withstood average beam currents of 50 mμA over a 0.1-cm² area without appreciable distortion. The effect of the target nonuni-

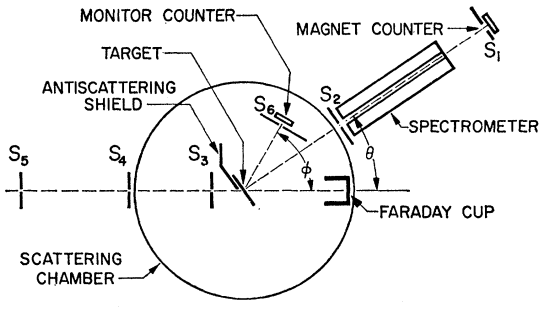

FIG. 1. Schematic diagram of equipment used for the $p+D$ breakup measurements.

[9] W. Heckrotte and M. MacGregor, Phys. Rev. **111**, 593 (1958).
[10] V. Komarov and A. Popova, Nucl. Phys. **18**, 296 (1960).
[11] A. Migdal, Zh. Eksperim. i Teor. Fiz. **28**, 3 (1955) [translation: Soviet Phys.—JETP **1**, 2 (1955)].
[12] K. Watson, Phys. Rev. **88**, 1163 (1952).
[13] B. Rybakov, V. Sidorov, and N. Vlasov, Nucl. Phys. **23**, 491 (1961).
[14] S. Kikuchi, J. Sanada, S. Wuwa, I. Hayashi, K. Nisimura, and K. Fukunaga, J. Phys. Soc. Japan **15**, 748 (1960).
[15] K. Nisimura, J. Phys. Soc. Japan **16**, 2097 (1961).
[16] C. Browne and W. Buechner, Rev. Sci. Instr. **27**, 899 (1956).
[17] G. Reid, J. Sci. Instr. **30**, 210 (1953).
[18] J. Allred, A. Armstrong, R. Bondelid, and L. Rosen, Phys. Rev. **88**, 433 (1952).

formity on the calculation of the differential cross section was small and will be discussed in Sec. III. A second target, about twice as thick and less uniform than the first, was also used. Proton spectra measured with both targets had essentially the same shape. Small differences in the shape near the low-energy end of the spectra were due to target thickness effects which will also be discussed in Sec. III.

Both targets were checked for contaminants by observation of the elastic scattering of protons at 90°. The only contaminant found was O^{16}, resulting from oil deposits on the target. The amount of C^{13} normally found in natural carbon (about 2%) was observed by studying the inelastic scattering of protons in the region of the known levels of C^{13}. Background runs were made with no target and with a $(CH_2)_n$ target prepared from commercial polyethylene sheet. The $(CH_2)_n$ target also contains C^{13} and about the same amount of oil contamination as the CD_2 target, and therefore the effect of these contaminants was easily taken into account.

The pulses from the CsI counter on the magnetic spectrometer, after amplification, were routed to a 100-channel pulse-height analyzer. The output from the monitor counter used in the experiment was split into three branches, one going to an integral discriminator and the other two to differential discriminators. The outputs from these discriminators went to three separate scalers. The integral discriminator was set to record only those protons elastically scattered from carbon, and the other two were set for the protons elastically scattered from deuterium and hydrogen.

The beam current entering the Faraday cup was integrated by an Elcor model A309A current integrator whose absolute accuracy is about 1%.

III. DATA ANALYSIS

The number of particles, N, recorded in the energy interval ΔE(MeV), by a detector of solid angle Ω, is given by the equation

$$N=3.76\times10^{6}(\rho XA/M)(Q/z)(d^2\sigma/d\Omega dE)(\Delta E)\Omega, \quad (1)$$

where ρX is the target thickness in mg/cm^2, M is the molecular weight of the target material, A is the number of atoms/molecule, z is the charge number of the incident particle, Q is the charge, in μC, collected by the Faraday cup, and $d^2\sigma/d\Omega dE$ is the differential cross section in mb/(sr-MeV).

A measurement of the effective target thickness by the usual area and weight measurements was not appropriate for two reasons. First, the amount of deuterium in the target decreased under bombardment while the amount of carbon did not; and second, the CD_2 targets contained a rather large amount (about 10%) of CH_2. Instead of using a direct measurement of the target thickness, a monitor counter was employed to measure the yield of protons from the p+D elastic scattering reaction. The known differential cross sections for this process (which were measured with gas targets) were then used to determine the target thickness term $(\rho XA/M)$. The determination of the differential cross section for the breakup reaction consisted then in measuring the ratio N/N_m, where N_m is the number of monitor counts.

The p+D elastic-scattering cross sections were determined from an interpolation of the data of Allred *et al.*[18] and Kikuchi *et al.*[19] The accuracy of the p+D elastic-scattering data is quoted to be 2–3%, and we believe that the accuracy of the interpolated values is better than 7%. Several monitor angles were used for each incident proton energy as a check for any inconsistencies in the extrapolated values of the p+D elastic cross sections. The values of the cross sections used for calculating the final results are shown in Table I.

The calculation of the magnet solid angle was complicated by the fact that different points on the target subtended different solid angles, and each point had to be weighted by the target thickness and beam density at that point. The effective solid angle for any size target spot was determined by a simple geometrical calculation assuming a uniform target thickness. The correction to the data concerning the nonuniformity of the target or beam density was estimated to be less than 5%, and we have taken this value as a measure of the uncertainty in the absolute value of the effective solid angle. The error in Ω due to a geometrical misalignment of the magnet was less than 0.5%.

The energy of the incident beam was determined by using the spectrometer to observe protons elastically scattered from a 0.0005-in. nickel target. The incident energy was then found from the measurement of the energy of the elastic peak, and from the known scattering angle. Several measurements at different energies indicated that the cyclotron frequency was a good measure of the beam energy and this measure was used in the remaining parts of the experiment. The measurements also indicated that the energy spread of the incident beam was about 1%. Since the differential cross section is not a rapidly varying function of the energy, this energy spread had a negligible effect on the measurements of the breakup spectra.

The width, W, of slit S_1 was $\frac{7}{8}$ in. corresponding to an energy resolution $(\Delta E/E)$ of 1.2%. The target angle

TABLE I. p+D elastic-scattering cross sections, $d\sigma_{el}/d\Omega$ (mb/sr), used in determining the effective deuterium target thickness.

	E_0 (Incident proton energy, MeV)			
φ(Lab scattering angle)	10.62	9.19	6.97	5.53
34.0	206	229	284	316
37.9		201		
41.9	158	174		
52.0	105	119	150	171

[19] S. Kikuchi, J. Sanada, S. Suwa, I. Hayashi, K. Nisimura, and K. Fukunaga, J. Phys. Soc. Japan **15**, 9 (1960).

was always set equal to the scattering angle so that the protons from the breakup would lose a minimum amount of energy in escaping the target.

Figure 2 shows some typical data from the magnet counter as recorded on a 100-channel pulse-height analyzer. The neutron-gamma background appears as an exponentially decreasing function of the energy. The peaks for the 1.5-MeV protons were always well resolved, but those for 1.0 MeV were well resolved only for the lower incident proton energies. The most difficult case to resolve was the 1.0-MeV yield for an incident proton energy, E_0, of 10.6 MeV. As many as six runs were taken for the poorly resolved peaks, and the error assigned to these points was taken to be the maximum discrepancy between all the runs. The error assigned to the well resolved peaks was the usual statistical factor.

Typical data of N versus spectrometer magnetic field (plotted in terms of the NMR frequency) are shown in Fig. 3. The CH_2 background in the regions away from the inelastic peaks is due to an accumulation

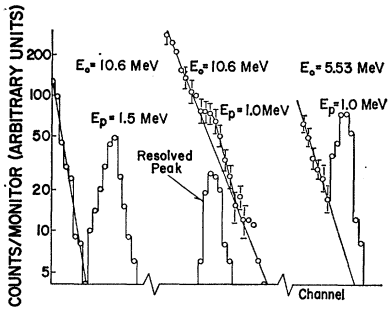

FIG. 2. Typical data from the magnet counter as recorded on a 100-channel pulse-height analyzer.

of low-energy "tails" resulting from higher energy proton groups, and also to those protons in the incident beam which are scattered by the entrance slits and then elastically scattered by the target. The broad peak in the CH_2 data between 10 and 13 Mc/sec is probably due to the $p+C^{12}\rightarrow p+3\alpha$ reaction. The alpha particles from this reaction and from the competing reaction $p+C^{12}\rightarrow \alpha+Be^9$ ($Be^9\rightarrow p+2\alpha$) were observed and easily distinguished from the protons of equal energy because of the difference in scintillation response of the CsI detector to alphas and protons. To correct the CD_2 data for the effects of these background events the CH_2 data were appropriately normalized for the differences in target thickness.

The presence of the excited levels of C^{12} was an unfortunate consequence of using a CD_2 target. However, because of the good energy resolution of the spectrometer, the peaks in the yield of protons from these excited states mask only a small portion of the breakup spectrum. Accordingly, these regions have been omitted in the calculation of the final results.

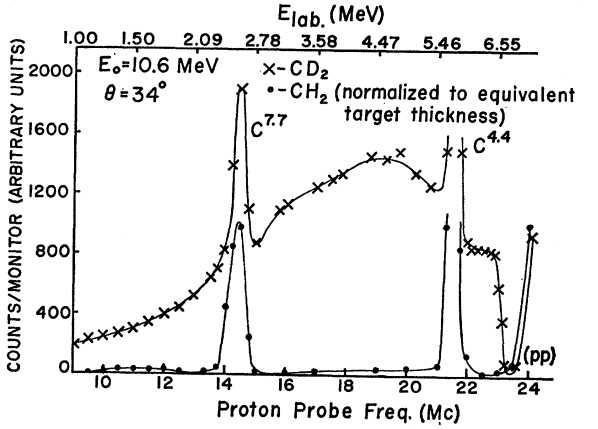

FIG. 3. Number, N, of protons from the CD_2 and CH_2 targets as a function of proton momentum (proportional to frequency). To obtain the differential cross section $N(CD_2-CH_2)$ has to be divided by $\Delta E\propto E\propto$ (frequency)^2.

The finite target thickness had two effects upon the shape of the spectrum. First, because of multiple scattering in the target, the protons which emerge from the target at an angle θ, were actually produced at some other angle. The rms multiple scattering angle for 1-MeV protons passing through 0.0005 in. of CD_2 is only 2°, and since the differential cross section is not a rapidly fluctuating function of the angle, we would expect that any corrections due to multiple scattering would be small. This was verified experimentally by the fact that the measured spectra were essentially independent of target thickness; the only differences occurred at low energies and these are explained by the second effect.

The second effect is due to the energy lost by the protons in passing through the target. The protons which emerge from the target with energy E were actually produced with different energies, the value depending upon the depth in the target at which the reaction occurred. A correction for this effect can be derived as follows. Let $f(E)$ be the true differential cross section and $f'(E)$ the measured one. Then, if t is the thickness of the target, we can write

$$f'(E)=\left(\frac{1}{t}\right)\int_0^t f[E+\Delta E(x)]\,dx,$$

and

$$f[E+\Delta E(x)]=f(E)+(\partial f/\partial E)\Delta E(x)+\cdots.$$

Now,

$$\Delta E(x)=\int_0^x\left(\frac{dE}{dx}\right)dx\simeq\left(\frac{dE}{dx}\right)x.$$

This approximation for ΔE is accurate to 5%, even for 1-MeV protons passing through a 0.0005-in. CD_2 target. It follows, after some simple algebra, that

$$f(E)\simeq f'(E)-(df/dE)(dE/dx)_{t/2}(t/2).$$

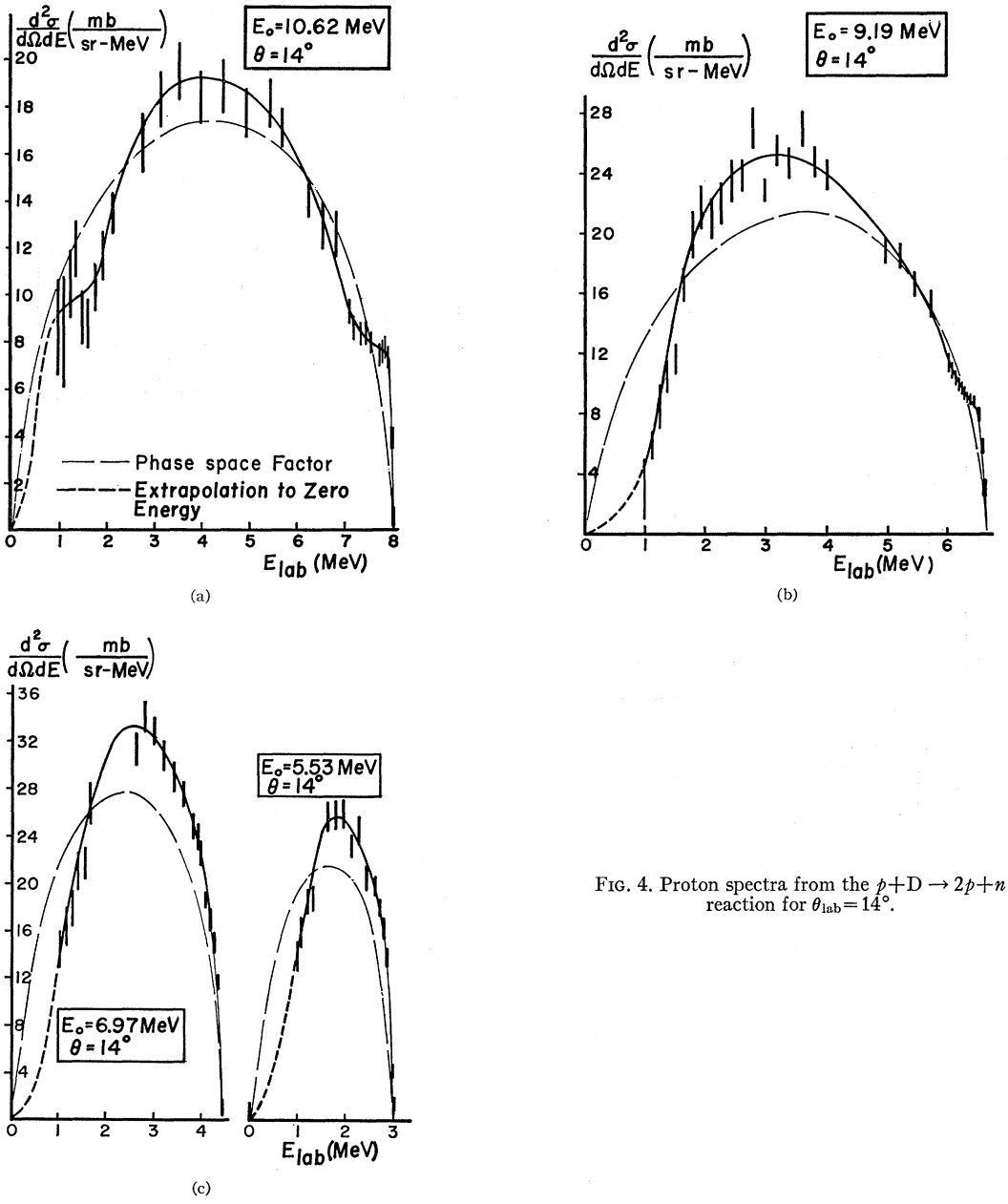

FIG. 4. Proton spectra from the $p+D \rightarrow 2p+n$ reaction for $\theta_{lab}=14°$.

This equation was evaluated for all the experimental curves using the range-energy tables of Rich and Madey.[20] The approximation $(df/dE)=(df'/dE)$ was used to calculate an initial value of $f(E)$ and then an iterative procedure was employed to obtain corrections to this value. The third term in the expansion of $f(E+\Delta E)$ was also evaluated and was found to be negligible.

IV. RESULTS

The results of the present experiment are shown in Figs. 4 and 5. The laboratory differential cross section for the production of protons is plotted as a function of the energy of the scattered protons for each incident energy E_0 and scattering angle θ. The experimental points have been corrected for the effects of the target thickness as explained in the previous section. At 1 MeV, the correction terms were less than 10% of the measured values for all the spectra except the $E_0=5.53$ MeV, $\theta=34°$ spectrum where it was 20% and the $E_0=9.19$ MeV, $\theta=14°$ spectrum where it was 50%. The correction terms become negligibly small at the maximum of the spectra and are less than 4% of the measured values for energies above the maximum. The errors shown are due to counting statistics. The uncertainty

[20] M. Rich and R. Madey, UCRL-2301, 1954 (unpublished).

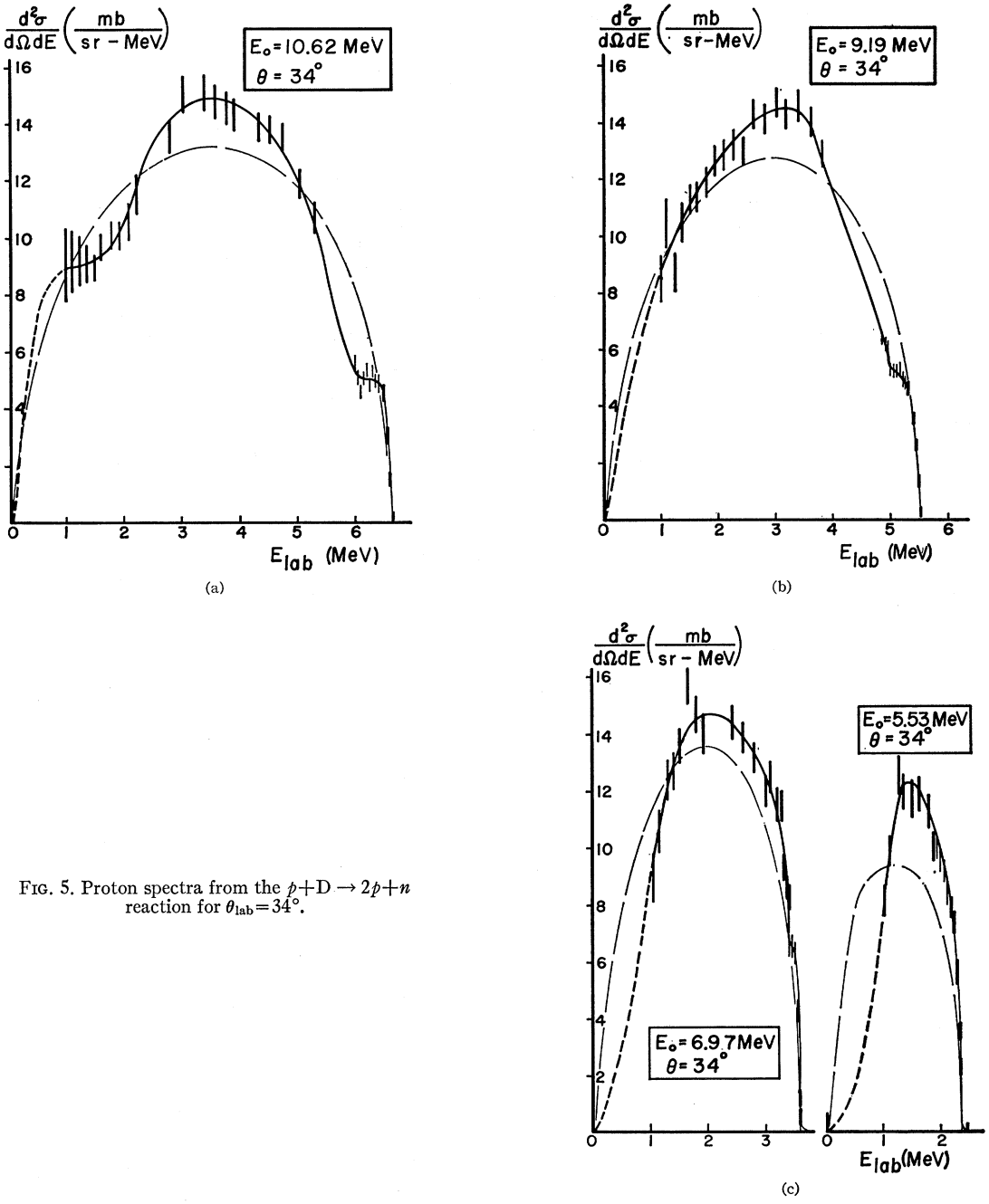

FIG. 5. Proton spectra from the $p+D \rightarrow 2p+n$ reaction for $\theta_{lab}=34°$.

in the absolute value of the differential cross sections depended largely on the uncertainties in Ω and in the elastic $p+D$ cross sections, and, consequently, is of the order of 10%. A plot of the phase-space factor (see Sec. V), normalized to equal the experimental area, is also shown for comparative purposes.

Although these proton spectra do not exhibit the double humped structure characteristic of the neutron spectra, there are several trends which should be noticed. All of the spectra have a rather steep slope at threshold, reaching one-third to one-half maximum height in less than a quarter of a MeV. The slope then decreases, the cross section rising to a maximum somewhere around $E/E_{max}=\frac{1}{2}$. The decrease of the differential cross section to zero is more rapid than that of the phase-space factor. It is evident that the observed spectra are displaced with respect to the phase-space factor toward higher energies. This shift is probably due to the effect of the Coulomb force in the final state.

The structure that appears at the high- and low-

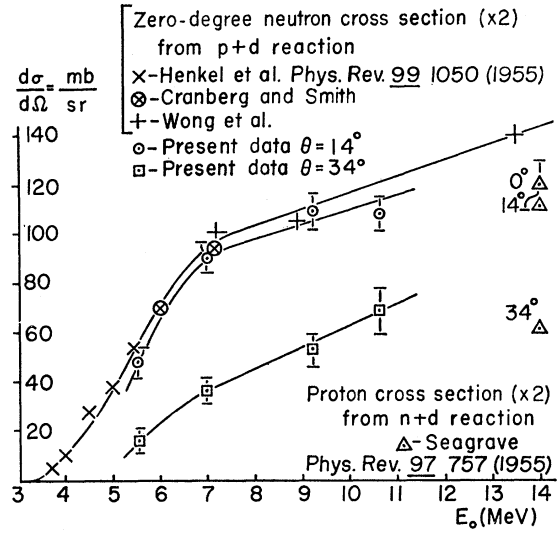

FIG. 6. The cross section for the production of protons from the $p+D \rightarrow 2p+n$ reaction as a function of incident proton energy.

energy ends of some of the spectra is due to the effects of final-state interactions. This structure becomes less pronounced as the incident energy decreases, and more pronounced as the scattering angle increases. These general characteristics are in good agreement with the observations of Kikuchi *et al.*[14] It should be noted that the lack of structure in the spectra for low-energy incident protons is not an indication that final-state interactions are unimportant, but rather that no one final state plays a more prominent role than any other. This is reasonable when we consider that, for an incident proton energy of $5\frac{1}{2}$ MeV, the maximum kinetic energy of any nucleon in the final state in the center-of-mass system is less than 1 MeV. At this low relative energy all three particles should be interacting strongly and one should not expect to see the effect of any one pair interaction.

The experimental data have been extrapolated to zero energy as shown on the graphs. The integral, from zero energy to $E_{\max}$, of the differential cross section has been plotted as a function of the incident proton energy E_0 in Fig. 6. The error assigned to the points of Fig. 6 was taken to be equal to the area under the extrapolated curve of the spectra. The cross section for the production of neutrons (multiplied by a factor of 2) has also been drawn on the graph. This correction factor is needed because two protons are produced for every neutron. However, the factor of 2 is not strictly correct, for although the total cross section for proton production is exactly twice that for neutrons, there is no reason why the cross section at any angle should differ by the same factor.

Gammel[7] found the cross section for the emission of protons at an angle of 34° with energies greater than 1.3 MeV to be 51 mb/sr at 9.66-MeV incident energy. The corresponding values for the present data are 46 mb/sr at 9.2 MeV, and 60 mb/sr at 10.6 MeV. A linear extrapolation to 9.66 MeV gives the value of 50 mb/sr in excellent agreement with Gammel's result. Similarly, Kikuchi *et al.*,[14] for 10.1-MeV incident energy, evaluate the cross section for the yield of protons with energy greater than 3.5 MeV, and find values of 80 mb/sr for 14°, and 20 mb/sr for 34°. Again, our result of 28 mb/sr at 34° is in excellent agreement; however, our result of 63 mb/sr at 14° differs considerably. As the experimental uncertainty quoted by Kikuchi *et al.* is ±5, and ours is ±2 mb/sr, it is difficult to reconcile these two values.

V. THEORETICAL CONSIDERATIONS

The differential cross section in the center-of-mass system is given by the familiar formula

$$\frac{d^2\sigma^*}{d\Omega^* dE^*} = \left(\frac{2\pi}{v^*}\right)\rho(E^*)\sum_{\text{spin}}|T|^2. \tag{2}$$

The density of final states for three particles of equal mass is given by

$$\rho(E^*) = (\tfrac{2}{3}E^*K - E^{*2})^{1/2}, \tag{3}$$

where E^* is the energy of the nucleon in the center-of-mass system, and K is the amount of energy in the center-of-mass system above the threshold for the breakup reaction. v^* is the velocity of the incident nucleon in the c.m. system, and T is the nuclear matrix element. Equation (3) transformed to the laboratory system and normalized to equal the experimental areas has been plotted in Figs. 4 and 5.

Consider the $p+D \rightarrow 2p+n$ reaction labeling the incident proton as "1" and the neutron and proton initially in the deuteron as "2" and "3," respectively. Let T_j be the usual kinetic energy operator and V_{jk} represent the interaction potential between the nucleons j and k. Then the T matrix for this reaction may be written in any one of the following forms:

$$T = (\varphi_1\varphi_2\varphi_3|\, V_{12}+V_{13}+V_{23}|\Psi_i^+) \tag{4}$$

$$= (\varphi_1 X_{23}^-|\, V_{12}+V_{13}|\Psi_i^+) \tag{5}$$

$$= (\varphi_2 X_{13}^-|\, V_{21}+V_{23}|\Psi_i^+) \tag{6}$$

$$= (\varphi_3 X_{12}^-|\, V_{13}+V_{23}|\Psi_i^+) \tag{7}$$

$$= (\Psi_f^-|\, V_{12}+V_{13}|\,\varphi_1 X_d). \tag{8}$$

φ_j and X_{jk} are the solutions of the Schrödinger equations $T_j\varphi_j = E_j\varphi_j$, and $(H_{jk}+T_n)\varphi_n X_{jk} = E\varphi_n X_{jk}$, where $H_{jk} = T_j+T_k+V_{jk}$. X_d is the ground-state deuteron wave function. Ψ is the properly antisymmetrized total wave function of the three-particle system: $H\Psi = E\Psi$, where $H = T_1+T_2+T_3+V_{12}+V_{13}+V_{23}$.

Equations (5), (6), and (7) called the final-state interaction formulas. For example, the matrix element $\langle X_{12}\varphi_3|\, V_{13}|\Psi_i^+\rangle$ describes an initial state, Ψ_i, broken up by the potential V_{13} resulting in a strongly inter-

acting final state, X_{12}^-, and an outgoing plane wave, φ_3. The formal solution for Ψ_i^+ is

$$\Psi_i^+ = |\varphi_1 X_d\rangle + \frac{1}{E_i - \sum_i T_i - V_{23} + i\epsilon}(V_{12}+V_{13})|\Psi_i^+\rangle.$$

Expanding this equation in terms of the initial asymptotic state $|\varphi_1 X_d\rangle$ gives

$$\Psi_i^+ = |\varphi_1 X_d\rangle + (1/e)(V_{12}+V_{13})|\varphi_1 X_d\rangle + (1/e) \times (V_{12}+V_{13})(1/e)(V_{12}+V_{13})|\varphi_1 X_d\rangle + \cdots, \quad (9)$$

where $e = E - \sum_i T_i - V_{23} + i\epsilon$.

All of the theoretical calculations mentioned in the Introduction start with one or more of the above T-matrix formulas. Bransden and Burhop[6] use Eq. (5) with the distorted-wave approximation, $\Psi_i = X_d F_0$, where F_0 is the solution of the Schrödinger equation corresponding to motion of a particle in the mean field of the deuteron. The interaction potentials were taken to be Gaussian, and X_{23} singlet and X_{23} triplet were taken as appropriate "deuteron" continuum wave functions. Frank and Gammel[7] use the Born approximation $\Psi_i = X_d\varphi_1$ and delta function potentials in the same formula. This permits them to express the inelastic-differential cross section in terms of the known elastic cross sections. High-energy neutrons from the $p+D$ reaction should arise from the breakup of the deuteron by the interaction leading to a final p-p state. This contribution is not included in the Frank and Gammel theory. Heckrotte and MacGregor[9] emphasized this term by using Eq. (6) with the Born approximation, and while their results do fit the shape of the high-energy neutron peak, they do not fit the low-energy peak.

Komarov and Popova[10] have combined the calculations of Frank and Gammel and Heckrotte and MacGregor. They evaluated the matrix elements (4), (5), and (6) in the Born approximation for the region in which each should be most important. The magnitude of the differential cross section for each region then was normalized to the experimental data. The excellent agreement that they obtain between theory and experiment (better than 10% over the entire spectrum) is surprising only at first sight. As will be shown, the use of the final-state interaction formalism should lead to good fits to the data in the appropriate regions provided that the proper normalization is used.

In connection with the final-state interaction formalism it is useful to introduce the momentum q of one of the nucleons in the final state pair in the center-of-mass system of the two nucleons forming the pair. Also let E'' be the excitation energy of this pair ($E''=q^2/m$). Watson[12] has shown that under certain general conditions the T matrix is given by $T=$ constant $e^{i\delta}(\sin\delta)/q$, where $\delta=\delta(q)$ is the S-wave scattering phase shift and the "constant" is a constant only in the sense of being independent of q. The necessary conditions for the validity of this form of the T matrix are that the interaction be strong and attractive and confined to a short range of the order "b," and that the wavelength $\lambda=h/q$, corresponding to the motion of one of the nucleons in the final-state pair, be much greater than "b." Substitution of this expression for the T matrix into Eq. (2) for the differential cross section yields

$$\frac{d^2\sigma^*}{d\Omega^* dE^*} = C_1(\tfrac{2}{3}E^*K - E^{*2})^{1/2}\frac{1}{(q\cot\delta)^2+q^2}, \quad (10)$$

where we have also used the density of final states as given by Eq. (3). This form of the cross section applies to n-n and n-p final-state interactions. The n-p final-state wave function can be either singlet or triplet, whereas the final-state n-n, or p-p wave functions can only be singlet for S-wave scattering. We, therefore, have two "constants" at our disposal for an n-p pair and one each for an n-n or p-p pair. For the final state p-p pair, the form of the differential cross section is greatly complicated by the Coulomb interaction and will not be presented here (see Ref. 11).

Equation (10) is exactly the same as the one derived by Frank and Gammel[7] [Eq. (36a)], where their theoretical development led to values of the "constants," C_{np}^s and C_{np}^t, in terms of the elastic-scattering cross sections and the relative strength of the interaction potentials. The important point to realize is that Eq. (10) has a resonance type structure and will naturally lead to peaks in the differential cross section. Whether or not these peaks are actually present depends on the value of the "constant" and it is *this "constant" which comes from a detailed calculation of the breakup process*. Thus one should always expect to be able to find a reasonable fit to the experimental data by picking the appropriate normalization.

The usefulness of the final-state interaction formalism lies in the fact that *if* a peak is experimentally observed one can say which final-state interaction is most important, and hence, which one of the Eqs. (5), (6), or (7), it is best to use. The magnitude of the "constant" comes from the calculation of this matrix element, and therefore depends on the choice of interaction potentials and on the approximations made in the calculations. At the present time, no calculations exist which give both the shape and the magnitude of the observed spectra.

VI. COMPARISON WITH THEORY AND DISCUSSION

The 9.2 MeV, 34°, differential cross-section data from Fig. 5, have been redrawn as a function of $E/E_{\max}$, and are shown in Fig. 7 where they are also compared to the results of Frank and Gammel. For each final state of the three-body system there is an outgoing nucleon, referred to as the "scattered" nucleon, and a nucleon which comes from the final-state pair, referred to as the "ejected" nucleon in the Frank and Gammel paper.

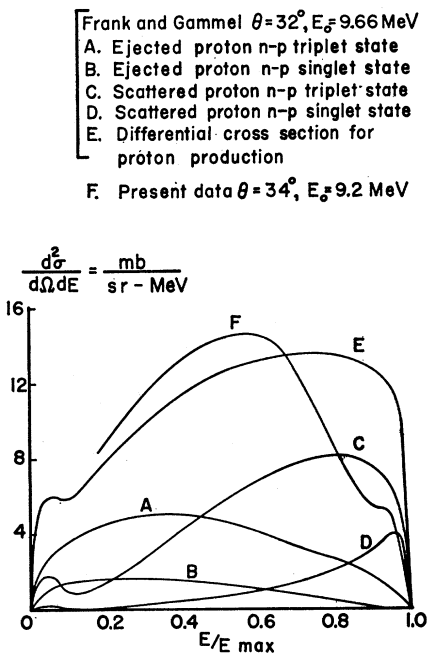

FIG. 7. Comparison between the observed differential cross section and that calculated by Frank and Gammel (Ref. 7).

Experimentally, it is impossible to distinguish which proton is detected; however, for purposes of calculation it is convenient to make this separation. Although the fit between the theoretical and experimental curves is rather poor, the comparison between them is interesting for several reasons. First, the Frank and Gammel curves indicate very clearly the energy region in which each type of final-state interaction is most important. The structure at the high-energy end of the spectrum shows quite obviously the effect of the singlet final state. The Frank and Gammel curves show that this peak is due to the singlet n-p final state. One would find contributions to this peak from both the singlet n-p and p-p states if a more detailed calculation were made. In this case, the p-p state refers to the interaction between the scattered proton and the proton in the n-p pair, and this interaction was neglected by Frank and Gammel. Since the final "deuteron" continuum state is a singlet state in this calculation, whereas the initial deuteron state is a triplet state, the incident proton has either exchanged with the proton in the deuteron, or one of the nucleons in the deuteron has had its spin flipped. A simple physical picture of the structure near the maximum breakup energy is the following. In the two-body p+D elastic scattering system, the scattered protons have a well-defined energy, which is just 2.33 MeV above the breakup threshold. If just enough energy is given to the deuteron to dissociate it, this peak "jumps" down 2.23 MeV, and since we now have a three-body system, the width of the peak will increase. Contributions from both the triplet and singlet states should be present, but since the resonance denominator, Eq. (10), is stronger for the singlet state we might expect it to dominate. This is true for energies E'' less than one-half MeV. Above this energy the triplet state, because of its greater statistical weight, begins to dominate. Therefore, one would expect to see the effects of the singlet state over a region of approximately one-half MeV below the maximum breakup energy.

The Frank and Gammel theory does not include the contribution from the p-p final state. If this state results from the n-p charge-exchange interaction, it will contribute two slow protons, whereas the same state formed as a result of a p-p pickup process will lead to intermediate-energy protons. In any case, more low-energy protons should be observed than this theory predicts, which is in the right direction to improve the agreement between the experimental and theoretical curves. It has been pointed out[21] that the inclusion of multiple-scattering terms (higher order terms in the expansion of Ψ_i^+) would move the high-energy Frank and Gammel peak towards lower energies. Multiple scattering may produce a displacement of the triplet contribution with respect to the singlet which would reproduce the observed structure. Finally, it should be noted that the Frank and Gammel theory does not include any Coulomb corrections. Unfortunately, inclusion of this factor should make the agreement with the experimental data even worse.

The only result that clearly emerges from an inspection of the experimental curves is that no one final state dominates the scattering at these low incident proton energies. The sharp rise and subsequent structure is most likely the effect of the singlet n-p system. The broad central peak has contributions from all the possible final states. The small structure near the low-energy end of the 10.6-MeV spectra may be due to the effect of the p-p final state. Since a low-energy proton in the laboratory corresponds to backward scattering angles in the center-of-mass system, this p-p state is a result of the p-n charge exchange interaction.

ACKNOWLEDGMENT

We wish to thank Dr. S. Mukherjee for the many hours he spent with the authors discussing the theoretical aspects of this problem.

[21] Dr. S. Mukherjee (private communication).